J Solid State Electrochem (2010) 14:1487–1497
DOI 10.1007/s10008-009-0969-0

ORIGINAL PAPER

Poly(3-octylthiophene) and polystyrene blends thermally treated as coatings for corrosion protection of stainless steel 304

U. León-Silva · M. E. Nicho

Received: 27 August 2009 / Revised: 29 October 2009 / Accepted: 2 November 2009 / Published online: 3 December 2009

Abstract The effect of thermal annealing of poly(3-octylthiophene) (P3OT) and polystyrene (PS) blend coatings on the corrosion inhibition of stainless steel in a 0.5 M NaCl solution was investigated. P3OT was synthesized by direct oxidation of the 3-octylthiophene monomer with ferric chloride ($FeCl_3$) as oxidant. Stainless steel electrodes with mirror finish were coated with P3OT/PS blend by drop-casting technique. In order to study the temperature effect on the function like physical barrier against the corrosive species of P3OT/PS polymeric blend, the coatings were thermally annealed at three different temperatures (55 °C, 80 °C, and 100 °C). The corrosion behavior of P3OT/PS-coated stainless steel was investigated in 0.5 M NaCl at room temperature, by using potentiodynamic polarization curves, linear polarization resistance (LPR), and electrochemical impedance spectroscopy. The LPR values indicated that, at 100 °C, P3OT/PS coatings showed a better protection of the 304 stainless steel in 0.5 M NaCl; the corrosion rate diminished in two orders of magnitude with regard to the bare stainless steel. The superficial morphology of the coatings before and after the corrosive environment was researched by atomic force microscopy, optic microscopy, and scanning electronic microscopy. Morphological study showed that the increased temperature benefited the integration of the two polymeric phases, which improved the barrier properties of the coatings. The coating/metal adhesion and the coating thickness were evaluated. The temperature increases the adhesion degree coating/substrate; thus, the coating annealed at 100 °C showed the best adhesion.

Keywords Polymeric blends · Coatings · Poly(3-octylthiophene) · Polystyrene · Annealed · Stainless steel · Corrosion

U. León-Silva
Centro de Investigación en Materiales Avanzados,
Miguel de Cervantes 120, Complejo Industrial Chihuahua,
Chihuahua, Chihuahua, Mexico

M. E. Nicho (✉)
Centro de Investigación en Ingeniería y Ciencias Aplicadas,
UAEMOR,
Av. Universidad 1001, Col. Chamilpa,
62209 Cuernavaca, Morelos, México
e-mail: menicho@uaem.mx

Introduction

The most common way to prevent a metal from corroding or to retard its corrosion is to provide an impervious coating over it. If a perfect barrier layer is applied to the surface of a metal exposed to a corrosive environment, then neither oxygen nor water can reach its surface and corrosion will be prevented [1]. Coating of metal surfaces with polymeric materials is one of the commonly used methods to protect the metals from corrosion [2]. In the past decade, the investigations on polymer blends have intensified significantly because they offer a convenient alternative to developing totally new polymers. The ability to produce blends having a desired combination of properties of the individual components depends on the compatibility of the system [3]. Therefore, the proper design of polymer blends can provide materials with desired properties that cannot be provided by a single polymer material, allowing the polymer blends versatility in various applications [4]. Recently conjugated polymers have been noted to offer corrosion protection of metal surfaces. A review of this potential for conjugated polymers was published by McAndrew [5, 6]. It was noted that many references conclude that undoped conjugated polymers exhibit better corrosion protection, while a similar number concludes that doped conjugated polymers are superior. This may be due to the specific corrosion test protocol employed for corrosion

evaluation. Several attempts have been made to employ conjugated polymers in blends with non-conductive polymer to improve processability and mechanical strengths as well as the cost-reduction of the expensive conductive polymers [7, 8]. A recent study noted that as low as 1% polyaniline (emeradine base) incorporated in a crosslinked epoxy network gave corrosion protection in aqueous 3.5% NaCl environments [9]. The addition of poly(3-decylthiophene-2,5-diyl) to alkyd, epoxy, and polyurethane coatings gave improved corrosion resistance in marine environments at levels as low as 0.3 *w/w* [10]. Polyaniline incorporated in a vinyl resin coating showed corrosion protection in both acid and neutral media [11]. A comprehensive study reported corrosion results involving controls,

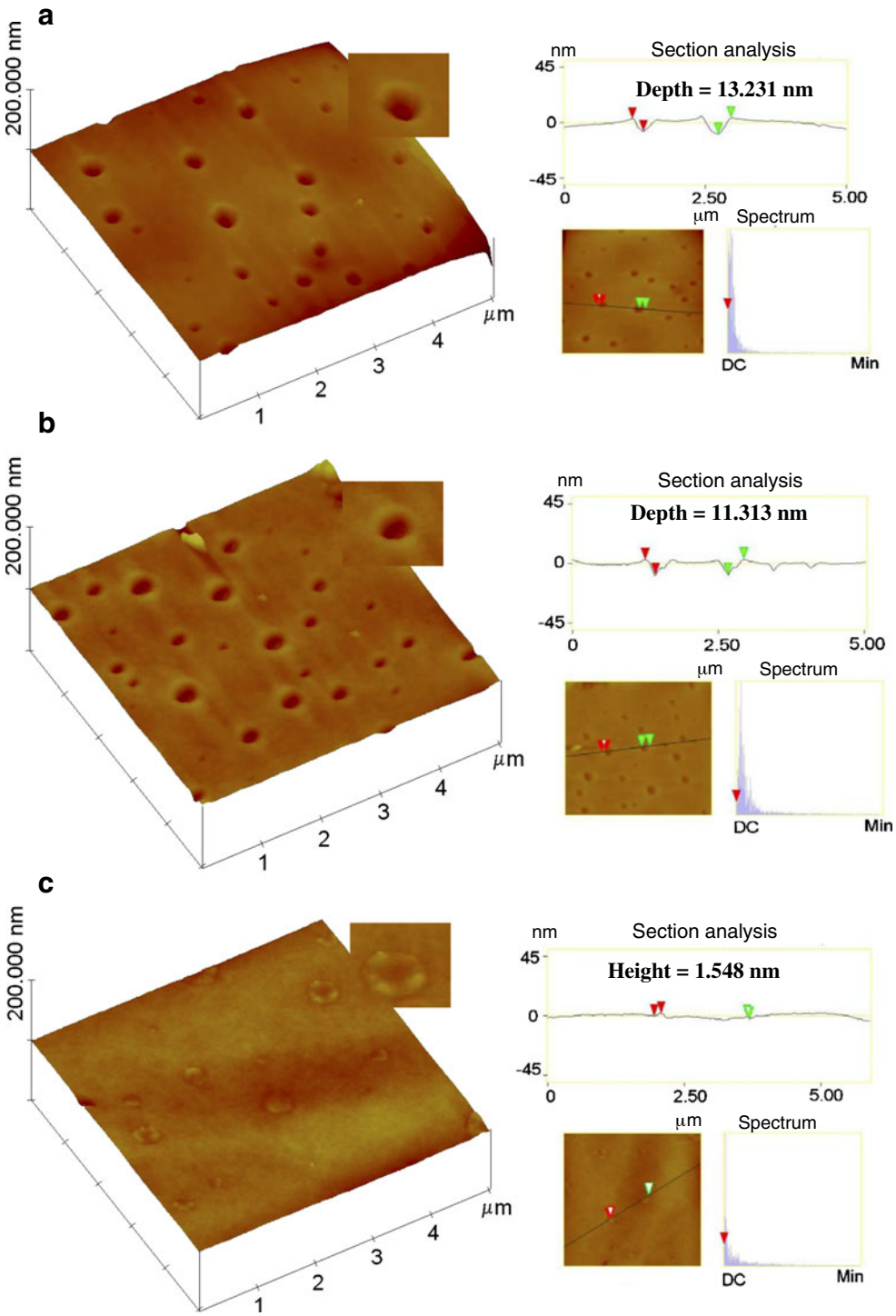

Fig. 1 AFM micrographs of 304SS substrates coated with P3OT/PS annealed at **a** 55 °C with roughness in Rms of 2.712 nm, **b** 80 °C with roughness in Rms of 1.333 nm, and **c** 100 °C with roughness in Rms of 1.141 nm

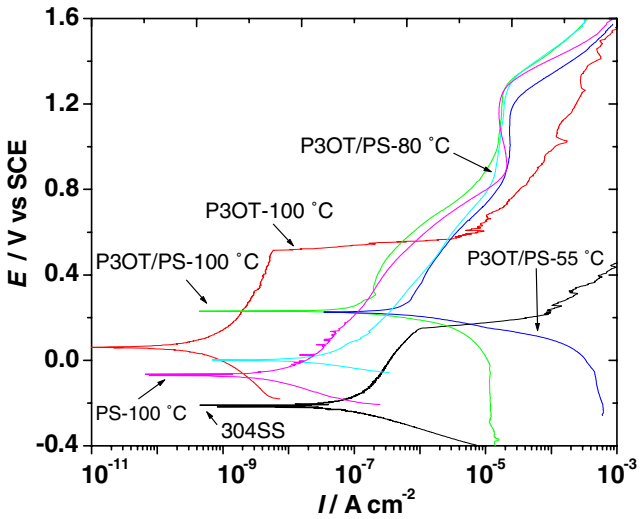

Fig. 2 Effect of annealing temperature on the polarization curves for 304SS uncoated and coated with P3OT/PS blends (annealed at 55 °C, 80 °C, and 100 °C) and PS and P3OT coatings annealed at 100 °C in 0.5 M NaCl

epoxy-coated steel, doped and undoped polyaniline top-coated with epoxy, and polypyrrole/polyurethane core-shell materials also topcoated with epoxy [7]. On the other hand, de Souza analyzed a blend of camphor sulphonate-doped polyaniline and poly(methyl methacrylate) used for iron, copper, and silver in acidic environments with or without chloride ions. These polymeric coatings showed good efficiency against metal corrosion [12]. da Silva and colleagues analyzed a blend composed by polyaniline (doped with two different dopants) and poly(methylmethacrylate). They found in all polymeric systems, potential values more positive than the potential of uncoated metals in acid solution, indicating the good protection of the metal substrate [13]. In another work, a heterogeneous blend of a soluble substituted polyaniline, poly(2,5-dimethoxy aniline) (PDMA), and two fluoropolymers, poly(vinylidene fluoride) and poly(tetra-fluoroethylene-*co*-vinylidene fluoride-*co*-propylene) were studied. The blends behave as an electrochemical barrier as well as a physical barrier showing superior corrosion inhibition in relation to PDMA [14]. The interest of conducting polymers for corrosion protection continues as the need for chromium-based corrosion-resistant coating replacement is a priority.

Among conjugated polymers, poly(3-alkylthiophene)s (P3ATs) are generating great interest to researchers because they are environmentally stable, easy to process, and have a wide range of electronic and optical properties which can be taken advantage of by modifying synthesis parameters. They are, therefore, suitable for application in various devices. P3ATs can be synthesized by both electrochemical and chemical polymerization techniques; however, it is easier to produce large amounts using chemical methods. Considering that poly(3-alkylthiophene)s with alkyl groups longer than butyl can readily be melt- or solution-processed into films [15], we decided to work with poly(3-octylthiophene) P3OT.

There have been attempts at the use of polythiophenes in anticorrosive applications. It was found that electrochemically deposited polythiophene coatings can provide corrosion protection of mild steel surfaces in 3.5% aqueous NaCl solution [16]. However, Rammelt et al. showed that the electrodeposition of P3MT films onto mild steel reduces the corrosion rate of mild steel even though they cannot passivate the metal surface in a 0.1 M NaCl solution [17].

Stainless steel type 304 has excellent corrosion resistance in a wide range of atmospheric environments and many corrosive media. However, pitting and crevice corrosion can occur in environments containing chlorides [18, 19]. On the other hand, P3OT is a soluble conducting polymer, but its mechanical property is bad and is also expensive. In this work, with the aim of overcoming these disadvantages to improve its use as coating of metals to prevent its corrosion, P3OT and polystyrene (PS) polymeric blends with thermal annealing applied as protective coatings to prevent the corrosion of type 304 stainless steel (304SS) were studied. Unfortunately, most of the blends containing conducting polymers have been found to be immiscible [20–22]. It is the case for the (polystyrene/poly(3-alkylthiophene) PS/P3AT blends [23–25]. The thermal annealing was carried out to improve the physical properties of polymeric blends with the aim of enhancing the barrier property of the polymeric coatings. Morphological changes in the coatings before and after corrosion tests were studied. Until now, there have been no reports related to the effect of thermal annealing on the corrosion performance of chemically polymerized soluble P3ATs in undoped/unoxidized state and its blends deposited on stainless steel in NaCl corrosive environments.

Experimental procedure

Materials

Commercial AISI 304SS sheets with 1 cm^2 of area were used in this study. Distilled 3-octylthiophene (3OT) monomer

Table 1 Electrochemical parameters obtained from polarization curves

Substrates	I_{corr} (Acm^{-2})	E_{corr} (mV)	E_{pit} and E_b (mV)
Uncoated 304SS	2.4×10^{-8}	−210	140
P3OT/PS (55 °C)	1.4×10^{-7}	219	1,220
P3OT/PS (80 °C)	1.6×10^{-8}	1.4	1,270
P3OT/PS (100 °C)	4.1×10^{-8}	226	1,270
P3OT (100 °C)	5×10^{-11}	50	500
PS (100 °C)	1.3×10^{-9}	−70	1,270

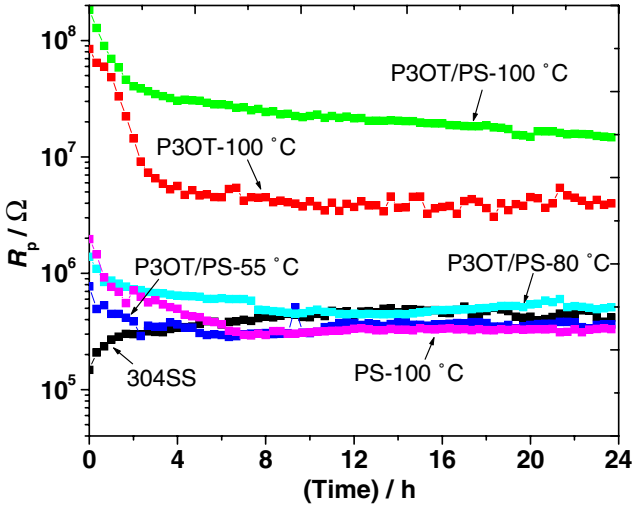

Fig. 3 Effect of annealing temperature on the change of R_p with time for the P3OT/PS-coated and bare 304SS samples in 0.5 M NaCl

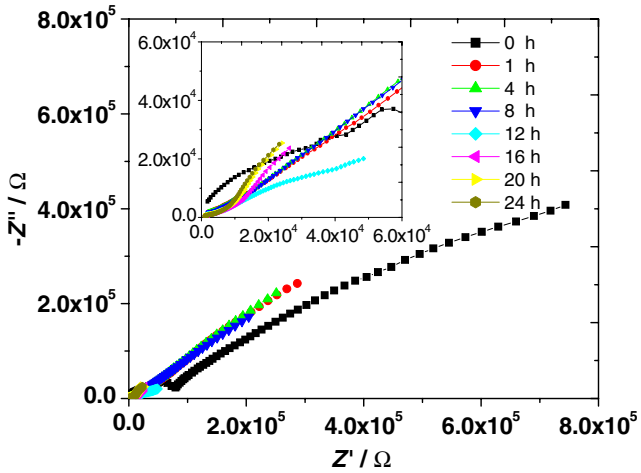

Fig. 5 Nyquist diagrams for 304SS coated with P3OT/PS annealed at 55 °C at different exposure times in 0.5 M NaCl

(Aldrich) was used for the synthesis of the polymer. The following were used without modification: ferric chloride ($FeCl_3$, 98%) (Aldrich), methanol (CH_3OH) (Fermont), chloroform ($CHCl_3$) (Baker), toluene ($C_6H_5CH_3$) (Aldrich), sodium chloride (NaCl) (Aldrich), hydrochloric acid (HCl) (Baker), acetone ($(CH_3)_2CO$) (Baker), and polystyrene ($(C_6H_5CH–CH_2)_n$) (Aldrich).

Electrodes

A 10-cm copper wire was welded to the steel sheet using thermocouple attachment unit equipment. Specimens with an exposure area of 10×10 mm were encapsulated with resin (MG 40 Crystal). Pre-treatment of the stainless steel substrates was carried out by polishing to a mirror finish (1.0 μ alumina) with different grades of emery papers. The substrates were washed with water, degreased with ethyl alcohol, and dried with warm air before the polymeric film coating process.

Chemical synthesis of the P3OT and preparation of the P3OT/PS blend

The P3OT polymer was synthesized by the chemical oxidative polymerization technique using ferric chloride ($FeCl_3$) as an oxidant and 3OT monomer in chloroform ($CHCl_3$) at room temperature in an inert atmosphere [26]. Anhydrous $FeCl_3$ (0.03835 mol) dissolved in $CHCl_3$ was slowly added to 0.0254 mol of 3OT dissolved in $CHCl_3$. The reaction mixture was stirred at room temperature for 25 h. The product was precipitated in methanol, filtered with a Buchner funnel, and washed three times with methanol, hydrochloric acid (10 vol.%), distilled water, and acetone. The precipitate was extracted with chloroform to isolate the

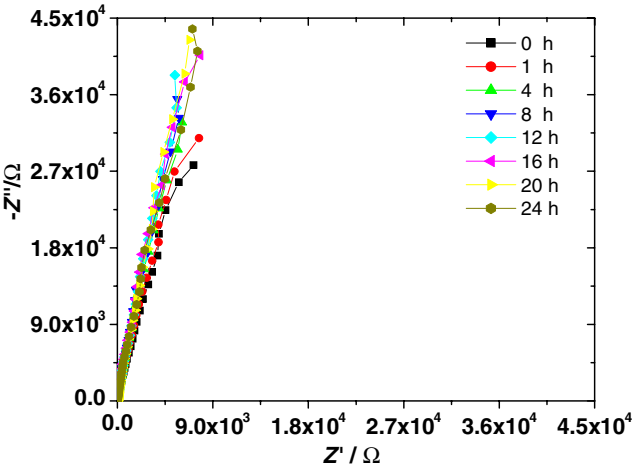

Fig. 4 Nyquist diagrams for bare 304SS at different exposure times in 0.5 M NaCl

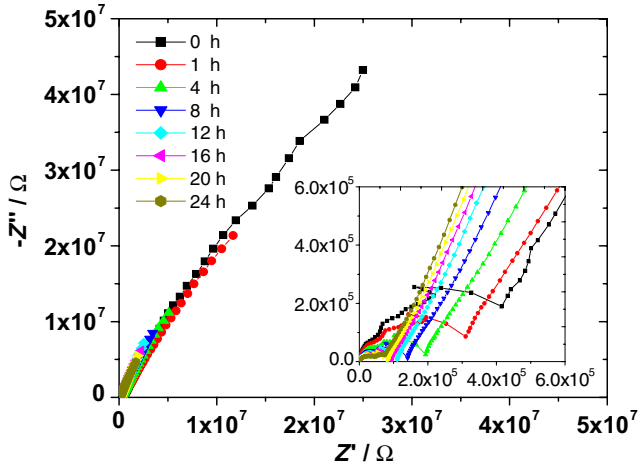

Fig. 6 Nyquist diagrams for 304SS coated with P3OT/PS annealed at 100 °C at different exposure times in 0.5 M NaCl

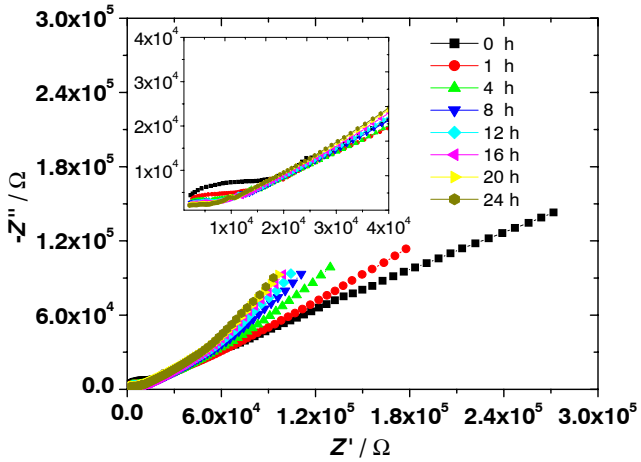

Fig. 7 Nyquist diagrams for 304SS coated with P3OT/PS annealed at 80°C at different exposure times in 0.5 M NaCl

chloroform-soluble fractions of the P3OT. Removal of the solvent resulted in red powders (pristine polymer).

For the preparation of the P3HT/PS polymeric blend, P3OT and PS were dissolved in toluene ($C_6H_5CH_3$) and stirred at room temperature for 1 h. The blend concentration was 80% PS and 20% P3OT.

The deposition process and thermal annealing

P3OT/PS coatings were deposited onto stainless steel sheets using the drop-casting technique. This technique consists of depositing a certain amount of polymeric solution (P3OT/PS in toluene, 12 drops as standard measurement) on the electrode, and when the dissolvent is evaporated, the coating is obtained. The polymeric solution was dried in a chamber with a toluene-saturated atmosphere. After the deposition process, the coatings were annealed in static air for 30 h at three different temperatures, 55 °C, 80 °C, and 100 °C.

Corrosion tests

Electrochemical experiments were carried out in a 0.5 M NaCl solution using a standard three-electrode cell with a coated or uncoated 304SS sheet as a working electrode, a saturated calomel electrode as a reference electrode, and a graphite rod as a counter electrode. The tests were performed at room temperature and controlled by a Gill AC serial no. 1340 automatized potentiostat. Polarization curves were conducted over the range −400 to 1,600 mV with respect to the free corrosion potential, E_{corr}, at a scan rate of 1 mV s^{-1}. Linear polarization resistance curves were obtained by sweeping the potential region between −10 and +10 mV with respect to the free corrosion potential, E_{corr}, at a scan rate of 1 mV s^{-1}, every 20 min for 24 h. Electrochemical impedance spectroscopy tests were carried out at E_{corr} using an AC potential amplitude of 10 mV, a frequency interval of 0.1 Hz to 30 kHz for 24 h, with 100 readings per decade.

The morphology of the polymeric coatings was examined before and after the corrosion tests with a Carl Zeiss DSM 960 series 6594 scanning electron microscope (SEM), a Nanoscope IV atomic force microscope (AFM, tapping mode) with a silicone nitride tip, and an Olympus GX71 optic microscopy.

Adhesion test and thickness measurement

The annealed coatings were cut in grid form. After this, a sticky tape was applied on the cut zone and pressed with a pencil eraser. The tape was taken off quickly, by raising the free end. The cut area was reviewed, and the loosening of the coating was evaluated. The ASTM 3359 norm was consulted regarding the experimental procedure and analysis of results.

The thickness of the coating was measured with a Mitutoyo brand digital micrometer. Three measurements were carried out for both bare and coated steel. The average value was determined in each case. Finally, the bare steel average thickness was subtracted from the polymer-coated steel average thickness.

Results and discussion

AFM micrographs

Figure 1 shows the P3OT/PS blend morphology annealed at (1) 55 °C, (2) 80 °C and (3) 100 °C. AFM images reveal

Table 2 Parameters used to simulate EIS data for bare 304SS in 0.5 M NaCl

Element	0 h	1 h	4 h	8 h	12 h	16 h	20 h	24 h
R_s Ω	8.5	8.5	8.6	8.5	8.4	8.6	8.7	8.5
CPE_{dl} Y_o ($\Omega^{-1}s^n$)	4.7×10^{-5}	4.3×10^{-5}	4.1×10^{-5}	3.7×10^{-5}	3.4×10^{-5}	3.2×10^{-5}	3.2×10^{-5}	3.1×10^{-5}
CPE_{dl} n	0.9	0.9	0.9	0.9	0.9	0.9	0.9	0.9
R_{ct} k Ω	195.3	218.2	274.7	350.9	408.3	392.7	428.2	373.5

evolution of blend morphology with temperature annealing. The micrographs showed pitted topography; the pits get continually shallower with the increase of temperature; it is, according with Ton-That et al. [27], who observed pitted topography in PS/PMMA blend, as the annealing process proceeds, the pits get continually shallower. In the present investigation, the depth of the pits decreased with the temperature from 13.231 nm (for 55 °C) to 11.313 nm (for 80 °C); however, in 100 °C, the pit-like morphology disappears, and the material inside the pit was elevated above the film surface until 1.548 nm. In previous work, we determined that, in P3OT/PS blends, films spin-cast from toluene and a phase segregation was formed with a lamellar structure: the bilayers with perforated upper PS lamella and P3OT bottom layer [25]; it is according to the previous report [23] that the same morphology was observed for PS/P3BT (1:1 *w*:*w*) films spin-cast from clorobenzene. In the micrographs (Fig. 1), it can be observed that the polymeric blend annealed to 55 °C showed the smooth upper phase; however, to increase the annealing temperature, this phase becomes increasingly rough (the P3OT/PS film annealed to 100 °C showed the granular morphology of P3OT inside and outside of the pits). Thus, the increased temperature benefited the integration of the two polymeric phases.

Thickness measurement and adhesion test

The thickness of the coatings was 58.6 μm for the blend annealed at 55 °C, 55.3 μm for the blend annealed at 80 °C, and 56.3 μm for the blend annealed at 100 °C. According to the ASTM 3359 norm, the adherence is measured as 0B, 1B, 2B, 3B, and 4B, where 0B describes coatings with weak adherence and 4B describes those with high adherence. The blends annealed at 55 °C and 80 °C showed poor adherence, 0B, while the blend annealed at 100 °C showed very good adherence, 4B. The better adherence shown by the blend annealed at 100 °C was due to the increased softening of the blend and the improved physical interaction of the coating/metal interface.

Corrosion tests

The effect of the annealing temperature on the polarization curves for uncoated and P3OT/PS-coated 304SS after 1 h of exposure to 0.5 M NaCl is given in Fig. 2. Uncoated 304SS showed corrosion (E_{corr}) and pitting or breakdown (E_{pit} or E_b) potential values of −210 and 140 mV, respectively. The corrosion current density value for bare 304SS was 2.4×10^{-8} A cm^{-2}. When the substrate was coated, the E_{corr} values were shifted in the noble direction, reaching their highest value close to 226 mV for the substrate coated with P3OT/PS annealed at 100 °C. Blend annealed at 80 °C and 55 °C had an E_{corr} value close to 1.4

Table 3 Parameters used to simulate EIS data for P3OT-coated 304SS annealed at 55 °C in 0.5 M NaCl

Element	0 h	1 h	4 h	8 h	12 h	16 h	20 h	24 h
R_s k Ω	1.3	1.8	1.7	1.7	2	1.3	0.8	0.8
CPE_{coat} $Y_o(\Omega^{-1}s^n)$	1×10^{-7}	5×10^{-6}	6×10^{-6}	8×10^{-6}	2×10^{-7}	2×10^{-5}	2×10^{-5}	2×10^{-5}
CPE_{coat} n	0.5	0.3	0.3	0.3	0.2	0.2	0.3	0.3
R_{coat} k Ω	127.5	36.1	25	22	19.5	17.3	12.1	11
CPE_{dl} $Y_o(\Omega^{-1}s^n)$	$8\ 10^{-7}$	–	–	–	–	–	–	–
CPE_{dl} n	0.4	–	–	–	–	–	–	–
R_{ct} k Ω	2000	–	–	–	–	–	–	–
W R_w	–	6.3×10^5	5.8×10^5	5.5×10^5	7.2×10^4	5.9×10^4	5.2×10^4	4.8×10^4
s	–	5	5	7	3	5	4	3
α	–	0.4	0.4	0.4	0.3	0.5	0.5	0.5

and 219 mV, respectively. In order to verify that the blend annealed at 100 °C was the one that was offering E_{corr} nobler values, the substrate was coated with PS or P3OT annealed at 100 °C and the results were −70 and 60 mV, respectively, thus, the E_{corr} nobler values were given by the P3OT/PS blend. The lowest I_{corr} value was exhibited by P3OT coating, close to 1.0×10^{-10} A cm^{-2}, two orders of magnitude lower than uncoated 304SS. The blends annealed at 55 °C, 80 °C, and 100 °C had an I_{corr} value close to I_{corr} value for the bare steel. The E_{corr} and I_{corr} values were calculated by Tafel extrapolation. The active behavior was still present when the substrate was coated with P3OT/PS coatings. For the annealed coatings, the E_b value was approximately 1,200 mV, one order of magnitude higher than bare 304SS. All these results are shown in Table 1.

The change in the polarization resistant (R_p) value over time in 0.5 M NaCl solution for bare 304SS and for that coated with P3OT/PS annealed at different temperatures is given in Fig. 3. The P3OT/PS-coated 304SS annealed at 100 °C showed the lowest corrosion rate; the R_p values were two orders of magnitude higher than bare 304SS at all measured times. This case was giving evidence for effective barrier behavior of P3OT/PS coating against the attack of corrosive species. The R_p values for P3OT/PS treated at 55 °C, 80 °C, and 100 °C reached steady-state values approximately after 6 h. In the case of 3OT/PS, treated at 55 °C and 80 °C, it reached values similar to those shown by bare 304SS in the steady state. In the first 8 h, 304SS coated with P3OT/PS blend annealed at 80 °C showed higher R_p values than those annealed at 50 °C, PS annealed at 100 °C, and bare 304SS. For the case of P3OT-coated 304SS annealed at 100 °C, as was reported by León-Silva et al. [28], the R_p values were one order of magnitude higher than bare 304SS at all measured times after steady state. It is clear that the blend with PS benefited the barrier behavior of P3OT coating against the attack of corrosive species. For corrosion protection in the immersed case, the most significant positive effect observed (at least before breakdown) of pristine polymers blends is that they obstructed the diffusion of corrosive species. The best corrosion performance for all immersion times was for those blends annealed at 100 °C. This improved performance is perhaps due to the better integration of the two polymeric phases where pores and defects are diminished.

According to AFM micrographs, when the blends were heated, the pits tended to disappear due to a better integration of the polymers; thus, a denser surface was obtained. A denser surface is correlated with better barrier properties. The better corrosion performance of the blends annealed at 100 °C was due to their denser surface (Fig. 1c) through which the corrosive species had more difficulty diffusing and reaching the underlying metal. In this case, only barrier properties were tested in the corrosion performance. Thus, an effective barrier behavior of P3OT/PS coating against the attack of corrosive species was observed when the P3OT/PS coating was annealed at 100 °C. Recently, Lee and coworkers studied the miscibility between P3OT and PS [8]. They experimentally determined the phase diagram by turbidity measurement. The blends exhibited the upper critical solution temperature type phase behavior. To achieve this objective, they used P3OT with lower molecular weight (2,000–3,000) because with larger molecular weight (~20,000), they could not obtain the turbidity temperature experimentally before the thermal degradation temperature. In our investigation, we used P3OT and PS with larger molecular weight, ~60,000 and 280,000, respectively. According to AFM images of P3OT/PS blend annealed at 100 °C, the film showed tend to form a single phase. Considering the phase diagram, it is interesting increasing the temperature or decreasing the P3OT concentration until obtaining only one phase because the barrier property of the coating will be improved.

In order to better understand the corrosion protection mechanism that these polymeric films can offer, electro-

Table 4 Parameters used to simulate EIS data for P3OT-coated 304SS annealed at 80 °C in 0.5 M NaCl

Element	0 h	1 h	4 h	8 h	12 h	16 h	20 h	24 h
R_s k Ω	2	2.1	2.2	2.3	2	2.2	2	2
CPE_{dl} $Y_o(\Omega^{-1}s^n)$	4.9×10^{-8}	1.8×10^{-7}	6.4×10^{-7}	5.5×10^{-7}	1×10^{-6}	1×10^{-6}	1×10^{-6}	2×10^{-6}
CPE_{dl} n	0.6	0.5	0.4	0.4	0.3	0.3	0.3	0.3
R_{ct} k Ω	28	22.7	21.6	18.2	19.8	18.3	17.6	18.6
W R_w	7.8×10^{-5}	3.9×10^{5}	2.3×10^{5}	18.5×10^{5}	1.6×10^{5}	1.5×10^{5}	1.4×10^{5}	1.3×10^{5}
s	25	9	4	3	2	2	2	2
α	0.3	0.3	0.3	0.3	0.3	0.3	0.3	0.3

Table 5 Parameters used to simulate EIS data for P3OT-coated 304SS annealed at 100 °C in 0.5 M NaCl

Element	0 h	1 h	4 h	8 h	12 h	16 h	20 h	24 h
R_s k Ω	1.4	1.1	2.2	2.5	3.1	3.1	3.7	3.5
CPE_{coat} $Y_o(\Omega^{-1}s^n)$	3.5×10^{-9}	4.3×10^{-9}	6.8×10^{-9}	1.2×10^{-8}	2×10^{-8}	2.9×10^{-8}	3.4×10^{-8}	7×10^{-8}
CPE_{coat} n	0.8	0.7	0.7	0.6	0.6	0.6	0.6	0.5
R_{coat} k Ω	632.5	377.7	209.7	153.3	123.0	107.2	95.3	90.1
CPE_{dl} $Y_o(\Omega^{-1}s^n)$	1.9×10^{-8}	–	–	–	–	–	–	–
CPE_{dl} n	0.7	–	–	–	–	–	–	–
R_p Ω	3×10^{8}	–	–	–	–	–	–	–
W R_w	–	1×10^{8}	2×10^{7}	2×10^{7}	1.6×10^{7}	1.4×10^{7}	1.2×10^{5}	1×10^{7}
s	–	11	4.8	4.7	4.5	4.5	0.01	4.6
α	–	0.7	0.7	0.7	0.7	0.7	0.4	0.7

chemical impedance spectroscopy (EIS) was employed to quantify the difference in the corrosion protection obtained by the effect of thermal annealing of stainless steel coated with blends of P3OT/PS in 0.5 M NaCl aqueous solution. Impedance measurements provide information on both the resistive and capacitive behavior of the interface and make possible the investigation of the performance of a polymer coating as a protective layer against metal corrosion [29]. Figure 4 shows the Nyquist plots for uncoated 304SS at different immersion times in 0.5 M NaCl. A tendency to form a semicircle was observed; the diameter of semicircle is the charge transfer resistance (R_{ct}) value (195 kΩ for 0 h). R_{ct} value increases during exposure time of 24 h (373 kΩ). This increment is due to the fact that the corrosive acidic chloride ions do not penetrate the surface steel easily. P3OT/PS coatings annealed at 55 °C and 100 °C showed in the beginning (0 h) a depressed semicircle in high frequency region and a second semicircle in low–middle frequencies (Figs. 5 and 6). The first semicircle is due to the presence of the coating and the second due to the electrochemical double layer. The P3OT/PS annealed at 80 °C showed in all time, a depressed semicircle in high-frequency region and a straight line in low-frequency region (Fig. 7). The same behavior was observed in the other coating systems (annealed at 55 °C and 100 °C) for the next hours (1–24 h). R_{ct} value decreases during exposure time of 24 h. This decrease is due to a decrease in the resistance of P3OT/PS blends, resulting in increased capacitance. The straight line in low frequency is due to Warburg impedance, which indicates the resistance of coating against the diffusion of corrosive species in the coated electrode. P3OT/PS annealed at 100 °C exhibits a higher impedance value ($5\times10^{7}\Omega$) compared with uncoated ($2.8\times10^{4}\Omega$) and coated steel with P3OT/PS annealed at 55 °C ($9\times10^{5}\Omega$) and 80 °C ($3\times10^{5}\Omega$), which indicates the protective effect of coating annealed at 100 °C deposited in corrosive medium [30]. In addition, P3OT/PS annealed at 100 °C presented the higher R_{ct} values (see Tables 2, 3, 4, and 5). Therefore, this coating offers good corrosion protection in 0.5 M NaCl.

Equivalent electric circuits to simulate EIS data for uncoated and coated 304SS are given in Fig. 8. In this figure,

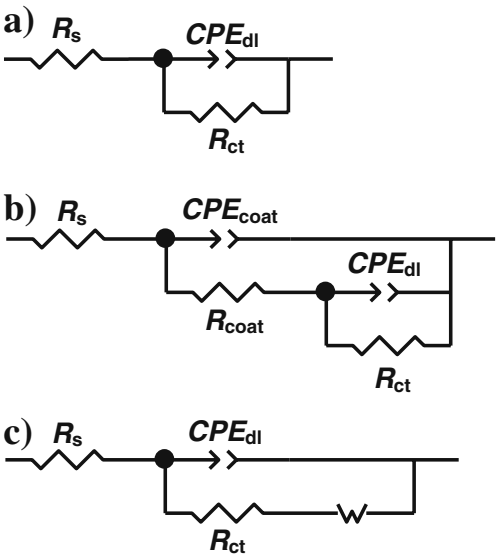

Fig. 8 Equivalent electric circuits to simulate EIS data for **a** bare 304SS, **b** coated 304SS with P3OT/PS annealed at 55 °C and 100 °C for 0 h, and **c** P3OT/PS annealed at 80 °C (all time) and 55 °C and 100 °C (for 1–24 h)

R_s is the medium resistance, and the ionic and electronic resistance of the polymer [31], C_{dl}, is the electrochemical double layer; R_{ct} is charge transfer resistance, C_{coat} is capacitance of coating, R_{coat} is coating resistance, and finally, W is Warburg impedance. In impedance spectroscopy practice, a number of experimental results show a frequency distribution of the parameters. The latter determined the necessity of a modeling element with frequency dispersion behavior. The constant phase element (*CPE*) which is distributed by its very nature is such an element [32]. The *CPE* is defined in impedance representation as

$$Z(CPE) = Y_o^{-1} = A(j\omega)^{-n} \quad (1)$$

where Y_o is the *CPE* constant, ω the angular frequency (in radians per second), $j^2=-1$ the imaginary number, and n is

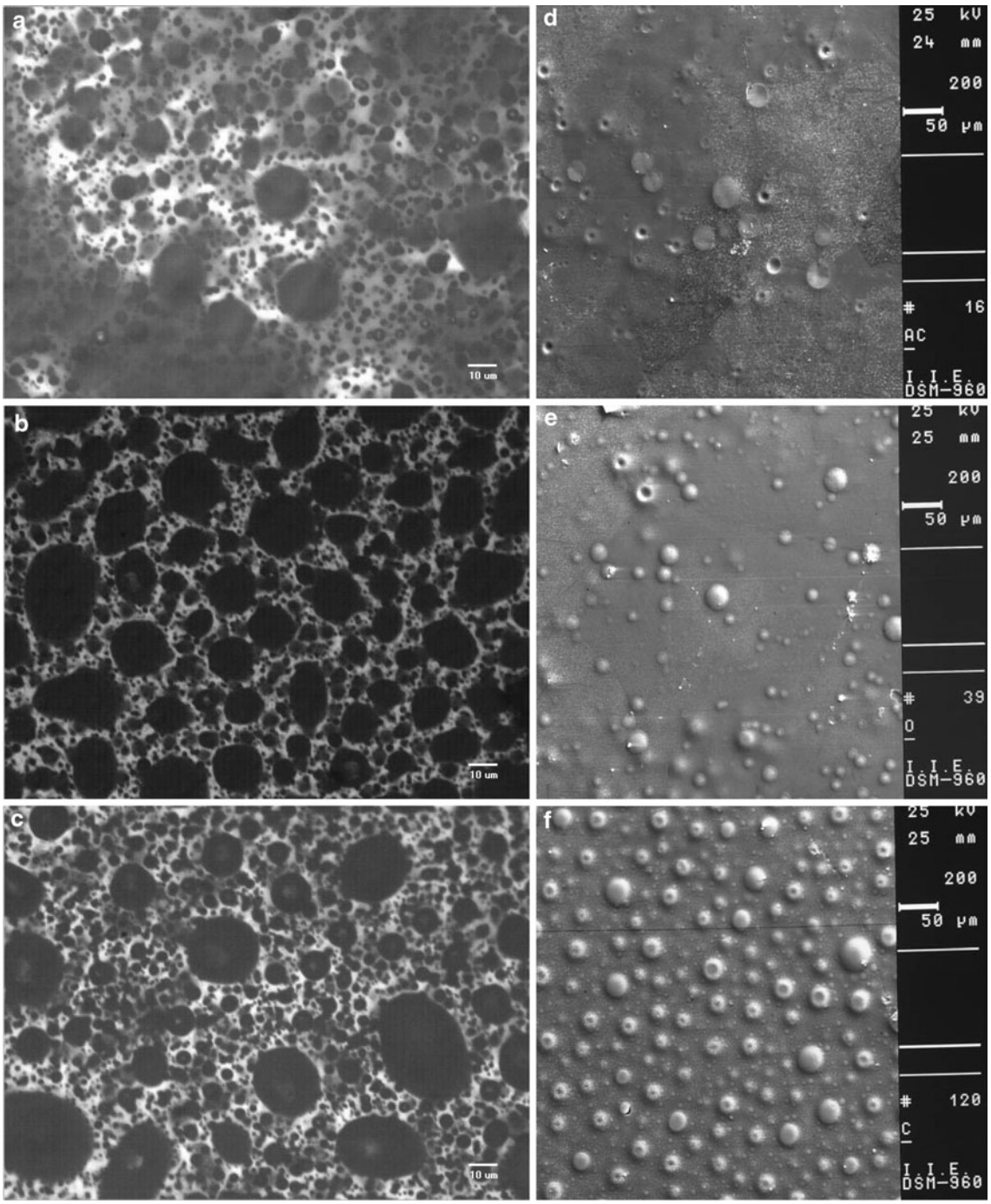

Fig. 9 Micrographs of 304SS substrates coated with P3OT/PS annealed at **a** and **d** 55°C, **b** and **e** 80°C, and **c** and **f** 100°C; **a**–**c** before the corrosion tests (optic microscopy images) and **d**–**f** after the corrosion tests (SEM images)

the *CPE* exponent. Depending on n, *CPE* can represent resistance ($Z(CPE)=R$, $n=0$), capacitance ($Z(CPE)=C$, $n=1$), inductance ($Z(CPE)=L$, $n=-1$) or Warburg impedance for ($n=0.5$) [33]. To describe the behavior of impedance spectra at low–middle frequencies, an exponent α is introduced in the expression for the Warburg impedance. Several models and expressions are used to describe this characteristic behavior of conducting polymer, but the finite–element Warburg impedance is expressed by:

$$Z_w = R_w(j\omega)^{\alpha} \quad (2)$$

were R_w is the modulus of the Warburg or diffusion resistance and α is the Warburg coefficient [34]. Calculated parameters used to simulate these impedance systems are given in Tables 2, 3, 4, and 5.

SEM micrographs

Figure 9a–c shows the optical micrographs of P3OT/PS blends coatings annealed at 55 °C, 80 °C, and 100 °C, respectively, before the corrosion test. These micrographs show a homogeneous surface morphology; they show that an increase of temperature benefited the integration of the two polymeric phases, as was indicated in AFM study. Figure 9d–f shows the SEM micrographs of these coatings after the corrosion test (24 h in 0.5 M NaCl solution). The results obtained in the corrosion tests were corroborated by SEM microscopy. In the case of the P3OT/PS, coating annealed at 55 °C (Fig. 9d) and at 80 °C (Fig. 9e); some holes and corrosion products were observed on the surface; however, the first case showed more holes that the second one, indicating higher degradation of the coating. However, the morphology of the P3OT/PS coating annealed at 100 °C (Fig. 9c) the film morphology was not amended.

Conclusions

The corrosion behavior of uncoated 304SS and P30T/PS blends coated 304SS annealed at three different temperatures (55 °C, 80 °C, and 100 °C) was investigated in 0.5 M NaCl. AFM images revealed evolution of blend morphology with temperature annealing; the polymeric films showed pitted topography. The pits get continually shallower with the increase of temperature and finally disappear. In comparison with the uncoated 304SS, polarization curves showed that the annealing of the polymeric coatings caused a change of E_{corr} values in the noble direction; however, the annealing did not benefit the I_{corr} value. The breakdown potential value was one order of magnitude higher than bare 304SS. Effect of annealing temperature on the change of R_p with time for the P3OT/PS-coated and bare 304SS samples in 0.5 M NaCl was studied. The results showed the lowest corrosion rate by using P3OT/PS-coated 304SS annealed at 100 °C; the R_p values were two orders of magnitude higher than bare 304SS at all measured times, therefore, this coating showed the best protection against corrosion of 304SS in NaCl medium. This case gave evidence of effective barrier behavior of P3OT/PS coating against the attack of corrosive species. This improved performance is perhaps due to the better integration of the two polymeric phases, where pores and defects are diminished, and a denser surface was obtained. EIS results showed that a Warburg-type impedance was observed, indicating that the corrosion mechanism was under mixed control: charge transfer from the metal to the environment through the double electrochemical layer and diffusion of aggressive ions through the polymeric coatings. The best corrosion performance was given by P3OT films annealed at 100 °C. AFM and optical microscope showed that the increase of annealing temperature benefited the density and the integration of the two polymeric phases. SEM showed that the coating annealing at 100 °C had the slightest degradation on the surface after the corrosion in NaCl medium.

Acknowledgements The authors thank Daniel Bahena Uribe for AFM images, Victor M. Salinas Bravo for SEM images, and Dr. Serna by the availability of the team for the corrosion proofs. The financial support from Consejo Nacional de Ciencia y Tecnología (CONACYT-México, 52598-R) is gratefully acknowledged.

References

1. Skotheim TA, Elsenbaumer RL, Reynolds JR (1998) Handbook of conducting polymers. Marcel Dekker Inc., New York
2. Ahmetli G, Kocak A, Sen N, Kurbanli R (2006) J Adhes Sci Technol 20:1431–1441
3. Caporaso L, Ludici N, Oliva L (2005) Macromolecules 38:4894–4900
4. Chen C, Wang J, Woodcock SE, Chen Z (2002) Langmuir 18:1302–1309
5. McAndrew TP, Miller SA, Gilicinski AG, Robeson LM (1996) PMSE Preprints 74:204–206
6. McAndrew TP (1997) TRIP 5:7–12
7. Robeson LM (2007) Polymer blends: a comprehensive review. Hanser, Germany
8. Lee Y, Kim JK, Chiu CH, Lan YK, Huang CI (2009) Polymer 50:4944–4949
9. Mari T, Anja T, Olof F, Olli I (2005) Polymer 46:6855–6861
10. Iribarren JI, Ocampo C, Armelin E, Liesa F, Alemán C (2008) J Appl Sci 108:3291–3297
11. Kamaraj K, Sathiyanarayanan S, Muthukrishnan S, Venkatachari G (2009) Prog Org Coat 64:460–465
12. de Souza S (2007) Surf Coat Technol 201:7574–7581
13. da Silva JEP, de Torresi SIC, Torresi RM (2007) Prog Org Coat 58:33–39
14. Moraga GA, Silva GG, Matencio T, Paniago RM (2006) Synth Met 156:1036–1042
15. Chen SA, Ni JM (1992) Macromolecules 25:6081–6089

16. Kousik G, Pitchumani S, Renganathan NG (2001) Prog Org Coat 43:286–291
17. Rammelt U, Nguyen PT, Plieth W (2001) Electrochim Acta 46:4251–4257
18. Galal A, Atta NF, Al-Hassan MHS (2005) Mater Chem Phys 89:28–37
19. Falleiros N, Wolynec S (2002) Mater Res 5:77–84
20. Vatansever F, Hacaloghlu J, Akbulut H, Toppare L (1996) Polym Int 41:237–244
21. De Paoli MA (1997) In: Naiwa HS (ed) Handbook of organic conductive molecules and polymers, vol 2. Wiley, New York
22. Narkis M, Zilberman M, Siegmann A (1997) Polym Adv Technol 8:525–528
23. Jaczewska J, Budkowski A, Bernasik A, Moons E, Rysz J (2008) Macromolecules 41:4802–4810
24. Babel A, Jenekhe SA (2004) Macromolecules 37:9835–9840
25. Nicho ME, Peña-Salgado D, Altuzar-Coello P (2009) Morphological and physicochemical properties of spin-coated poly(3-octylthiophene)/polystyrene composite thin films. Thin Solid Films. doi:10.1016/j.tsf.2009.09.036
26. Sugimoto R, Takeda S, Gu HB, Yoshino K (1986) Chem Express 1:635–638
27. Ton-That C, Shard AG, Daley R, Bradley RH (2000) Macromolecules 33:8453–8459
28. Silva UL, Nicho ME, Rodríguez JG, Nava JG, Bravo VMS (2009) Effect of thermal annealing of poly(3-octylthiophene) films covered stainless steel on corrosion properties. J Solid State Electrochem. doi:10.1007/s10008-009-0918-y
29. Maranhão SLA, Guedes IC, Anaissi FJ, Toma HE, Aoki IV (2006) Electrochim Acta 52:519–526
30. Yagan A, Pekmez NÖ, Yıldız A (2007) Poly(*N*–ethylaniline) coatings on 304 stainless steel for corrosion protection in aqueous HCl and NaCl solutions. Electrochim Acta. doi:10.1016/10.016
31. Conroy KG, Breslin CB (2003) Electrochim Acta 48:721–732
32. Popova A, Sokolova E, Raicheva S, Christov M (2003) Corros Sci 45:33–37
33. Sathiyanarayanan S, Azim SS, Venkatachari G (2007) Synth Met 157:205–213
34. Barsoukov E, Macdonald JR (2005) Impedance spectroscopy theory, experiment, and applications, 2nd edn. Wiley, New Jersey